

## BRIEF REPORT

# GCT-TTE: Graph Convolutional Transformer for Travel Time Estimation

Vladimir Mashurov<sup>1†</sup>, Vaagn Chopurian<sup>1†</sup>, Vadim Porvatov<sup>1,2†</sup>, Arseny Ivanov<sup>3</sup> and Natalia Semenova<sup>1,4\*</sup>

\*Correspondence:

[semenova.bnl@gmail.com](mailto:semenova.bnl@gmail.com)

<sup>4</sup>Artificial Intelligence Research Institute, Nizhniy Susalnyy Lane 5, 105064 Moscow, Russia

Full list of author information is available at the end of the article

<sup>†</sup>Equal contribution

## Abstract

This paper introduces a new transformer-based model for the problem of travel time estimation. The key feature of the proposed GCT-TTE architecture is the utilization of different data modalities capturing different properties of an input path. Along with the extensive study regarding the model configuration, we implemented and evaluated a sufficient number of actual baselines for path-aware and path-blind settings. The conducted computational experiments have confirmed the viability of our pipeline, which outperformed state-of-the-art models on both considered datasets. Additionally, GCT-TTE was deployed as a web service accessible for further experiments with user-defined routes.

**Keywords:** machine learning; graph convolutional networks; transformers; geospatial data; travel time estimation

## Introduction

Travel time estimation (TTE) is an actively developing branch of computational logistics that considers the prediction of potential time expenditures for specific types of trips [1, 2]. With the recent growth of urban environment complexity, such algorithms have become highly demanded both in commercial services and general traffic management [3]. Following this line, better TTE decreases logistic costs for different kinds of delivery [4], improves end-user experience for taxi services [5], and ensures the quality of adaptive traffic control [6].

Despite the applied significance of travel time estimation, it still remains a challenging task in the case of ground vehicles. This situation arises from the influence of different patterns of road network topology, nonlinear traffic dynamics, changing weather conditions, and other types of unexpected temporal events. The majority of the currently established algorithms [7, 8] tend to utilize specific data modalities in order to capture complex spatio-temporal dependencies influencing the traffic flow. With the recent success of multimodal approaches in adjacent areas of travel demand prediction [9] and journey planning [10], fusing the features from different sources is expected to be the next step towards better performance in TTE.

In this paper, we explored the predictive capabilities of TTE algorithms with different temporal encoders and proposed a new transformer-based model GCT-TTE. The main contributions of this study are the following:

- 1 In order to perform the experiments with the image modality, we extended the graph-based datasets for Abakan and Omsk [11] by the map patches (image modality) in accordance with the provided trajectories. Currently, the extended datasets are the only publicly available option for experiments with multimodal TTE algorithms.

**Table 1** Demonstration of utilized modalities in path-blind and path-aware models

Path-blind models				Path-aware models			
Model	Modality			Model	Modality		
	Graph	Images	GPS		Graph	Images	GPS
AVG	-	-	-	WDR	+	-	-
LR	-	-	-	DeepIST	-	+	-
MURAT	+	-	-	DeepTTE	-	-	+
DeepI2T	+	+	-	DeepI2T	+	+	-

- In order to boost further research in the TTE area, we reimplemented and published the considered baselines in a unified format as well as corresponding weights and data preprocessing code. This contribution will enable the community to enhance evaluation quality in the future, as most of the TTE methods lack official implementations.
- We proposed the GCT-TTE neural network for travel time estimation and extensively studied its generalization ability under various conditions. Obtained results allowed us to conclude that our pipeline achieved better performance regarding the baselines in terms of several metrics. Conducted experiments explicitly indicate that the performance of the transformer-based models is less prone to decrease (in the sense of the considered metrics) with the scaling of a road network size. This property remains crucial from an industrial perspective, as the classic recurrent models undergo considerably larger performance dropdowns.
- For demonstration purposes, we deployed inference of the GCT-TTE model as the web application accessible for manual experiments.

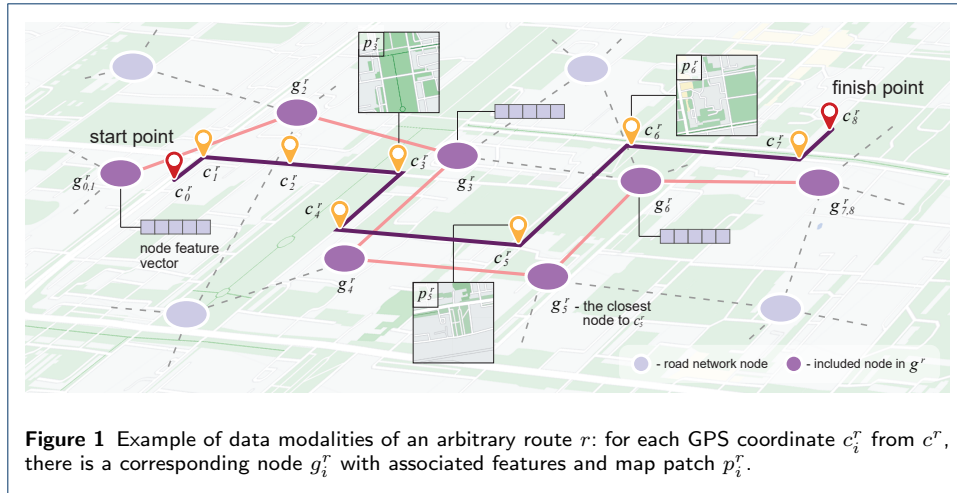
The web application is available at <http://gctte.online> and the code is published in the GitHub repository of the project<sup>[1]</sup>.

## Related work

Travel time estimation methods can be divided into two main types of approaches corresponding to the *path-blind* and *path-aware* estimation, Table 1. The path-blind estimation refers to algorithms relying only on data about the start and end points of a route [12]. The path-aware models use intermediate positions of a moving object represented in the form of GPS sequences [13], map patches [14], or a road subgraph [7]. Despite the computational complexity increase, such approaches provide significantly better results, which justify the attention paid to them in the recent studies [15, 8, 16].

One of the earliest path-aware models was the wide-deep-recurrent (WDR) architecture [17], which mostly inherited the concept of joint learning from recommender systems [18]. In further studies, this approach was extended regarding the usage of different data modalities. In particular, the DeepIST [14] model utilizes rectangular fragments of a general reference map corresponding to elements of a route GPS sequence. Extracted images are fed into a convolutional neural network (CNN) that captures spatial patterns of depicted infrastructure. These feature representations

<sup>[1]</sup><https://github.com/Eighonet/GCT-TTE>



are further concatenated into the matrix processed by the long short-term memory (LSTM) layer [19].

In contrast with the other approaches, DeepTTE [20] is designed to operate directly on GPS coordinates via geospatial convolutions paired with a recurrent neural network. The first part of this pipeline transforms raw GPS sequences into a series of feature maps capturing the local spatial correlation between consecutive coordinates. The final block learns the temporal relations of obtained feature maps and produces predictions for the entire route along with its separate segments.

The concept of modality fusing was first introduced in TTE as a part of the DeepI2T [21] model. This architecture uses large-scale information network embedding [22] to produce grid representations and 3-layer CNN with pooling for image processing. As well as DeepTTE, DeepI2T includes the segment-based prediction component implemented in the form of residual blocks on the top of the Bi-LSTM encoder.

In addition to extensively studied recurrent TTE methods, it is also important to mention recently emerged transformer models [23, 24]. Despite the limited comparison with classic LSTM-based methods, they have already demonstrated promising prediction quality, preserving the potential for further major improvements [25, 26]. As most of the transformer models lack a comprehensive evaluation, we intend to explore GCT-TTE performance with respect to a sufficient number of state-of-the-art solutions to reveal its capabilities explicitly.

## Preliminaries

In this section, we introduce the main concepts required to operate with the proposed model, Figure 1.

**Route.** A route  $r$  is defined as the set  $\{c^r, a^r, t^r\}$ , where  $c^r$  is the sequence of GPS coordinates of a moving object,  $a^r$  is the vector of temporal and weather data,  $t^r$  is the travel time.

As the *image modality*  $p^r$  of a route  $r$ , we use geographical map patches corresponding to each coordinate  $c_i^r \in c^r$ . Each image has a fixed size  $256 \times 256 \times 3$  across all of the GPS sequences in a specific dataset.

**Table 2** Description of the Abakan and Omsk datasets.

Road network			Trips		
Property \ City	Abakan	Omsk	Property \ City	Abakan	Omsk
Nodes	65 524	231 688	Trips number	121 557	767 343
Edges	340 012	1 149 492	Coverage	53.3%	49.5%
Clustering	0.5278	0.53	Average time	427 sec	608 sec
Usage median	12	8	Average length	3604 m	4216 m

**Road network.** Road network is represented in the form of graph  $G = \{V, E, X\}$ , where  $V = \{v_1, \dots, v_n\}$  is the set of nodes corresponding to the segments of city roads,  $E = \{(v_i, v_j) \mid v_i \rightarrow v_j\}$  is the set of edges between connected nodes  $v_i, v_j \in V$ ,  $X : n \times m \rightarrow \mathbf{R}$  is a feature matrix of nodes describing properties of the roads' segments (additional information regarding available graph features is provided in Supplementary 1).

Description of a route  $r$  can be further extended by the *graph modality*  $g^r = \{v_k \mid k = \operatorname{argmin}_j \rho(c_i^r, v_j)\}_{i=1}^{|c^r|}$ , where  $\rho(c_i^r, v_j)$  is the minimum Euclidean distance between coordinates associated with  $v_j$  and  $c_i^r$ . Following the same concept as in the case of  $p^r$ , the graph modality represents a sequence of nodes and their features aggregated with respect to the initial GPS coordinates  $c^r$ .

**Travel time estimation.** For each entry  $r$ , it is required to estimate the travel time  $t^r$  using the elements of feature description  $\{c^r, p^r, g^r, a^r\}$ .

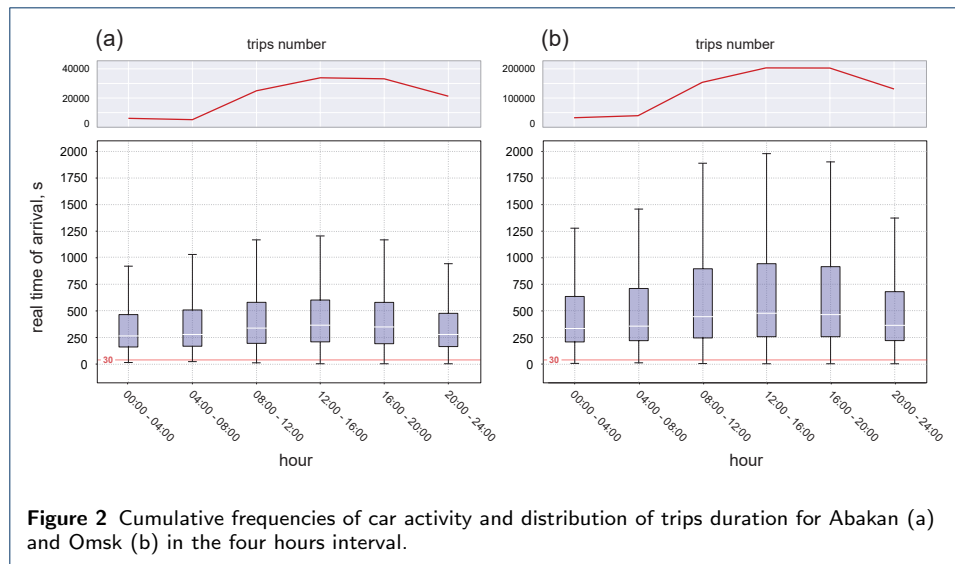
## Data

We explored the predictive performance of the algorithm on two real-world datasets collected during the period from December 1, 2020 to December 31, 2020 in Abakan (112.4 square kilometers) and Omsk (577.9 square kilometers). Each dataset consists of a road graph and associated routes, Table 2. In the preprocessing stage, we excluded trips that lasted less than 30 seconds (273, 0.22% for Abakan; 1194, 0.15% for Omsk) along with the ones that took more than 50 minutes (223, 0.18% for Abakan; 3681, 0.47% for Omsk). The distributional statistics of both datasets are depicted in Figure 2.

Since initial versions of Abakan and Omsk datasets did not have any relevant input data for image-based models, we extended their road graphs with the map patches parsed from Open Street Map (OSM)<sup>[2]</sup>. The parsing algorithm extracted patches from the OSM tile server URLs in accordance with the following request template: <http://a.tile.openstreetmap.org/{zoom}/{longitude}/{latitude}.png>. In order to utilize obtained data together with initial graphs, it was extended by mapping tables including the closest node id for each patch. The applied proximity measure was based on the Euclidean distance between location of image centroids and geographical coordinates of graph vertexes. Due to the limitations of the API throughput, the procedure of image extraction was distributed between several machines with a total execution time exceeding 1 week.

The provided extension consists of images dated July 2022: due to the absence of significant changes in the road network topology since 2020, image modality for

<sup>[2]</sup><https://www.openstreetmap.org>



Abakan and Omsk remains actual with respect to the original graph-based data. The content of the patches includes a full range of geographic objects useful for travel time estimation (e.g., road networks, landscape groups, buildings and associated infrastructural objects) and covers all of the routes provided in the initial datasets.

Depending on the requirements of the considered learning model, image datasets had to be organized regarding the fixed grid partitions or centered around the elements of GPS sequences. In the first case, a geographical map of a city was divided into equal disjoint patches, which were further mapped with the GPS data in accordance with the presence of coordinates in a specific partition. Trajectory-based approach to dataset construction does not require the disjoint property of images and relies on the extraction of patches with the center in the specified coordinate, Algorithm 1 (*collect* and *split* functions can be accessed in Supplementary 2-3). The obtained grid-based image dataset consists of 96 101 instances for Abakan and 838 865 for Omsk while the trajectory-based dataset has 544 502 and 3 376 294 images correspondingly.

One of the crucial features of the considered datasets is the absence of traffic flow properties. The availability of such data is directly related to the specialized tracking systems (based on loop detectors or observation cameras), which are not presented in the majority of cities. In order to make the GCT-TTE suitable for the greatest number of urban environments, we decided not to limit the study by the rarely accessible data.

## Method

In this section, we provide an extensive description of the GCT-TTE main components: pointwise and sequence representation blocks, Figure 3.

### Patches encoder

In order to extract features from the image modality, we utilized the RegNetY [27] architecture from the SEER model family. The key component of this architecture is

**Algorithm 1** Trajectory-based route preparation algorithm for image modality

---

```

1: result = [] ▷ [] – empty list
2: for path in paths do ▷ For each path
3:   route_centers = []
4:   i ← 0
5:   if len(path) == 1 then ▷ If path contents only one node
6:     result ← path
7:     continue
8:   end if
9:   while i + 1 < len(path) do ▷ len() – length
10:    centroids ← []
11:    k ← 1
12:    if ( $\rho(\text{path}[i], \text{path}[i + 1]) < 200$ ) then
13:      center, k ← collect(path, i)
14:      route_centers ← center
15:      i = i + k
16:      continue
17:    end if
18:    if  $\rho(\text{path}[i], \text{path}[i + 1]) \geq 200$  then
19:      for point in split(path[i], path[i + 1]) do
20:        route_centers ← point
21:      end for
22:    end if
23:    i = i + 1
24:  end while
25:  result ← route_centers
26: end for

```

---

the convolutional recurrent neural network (ConvRNN) which controls the spatio-temporal information flow between building blocks of the neural network.

Each RegNetY block consists of three operators. The initial convolution layer of  $t$ 'th block processes the input tensor  $X_1^t$  and returns the feature map  $X_2^t$ . Next, the obtained representation  $X_2^t$  is fed to ConvRNN:

$$H^t = \tanh(C_x(X_2^t) + C_h(H^{t-1}) + b_h), \quad (1)$$

where  $H^{t-1}$  is the hidden state of the previous RegNetY block,  $b_h$  is a bias tensor,  $C_x$  and  $C_h$  correspond to convolutional layers. In the following stage,  $X_2^t$  and  $H^t$  are fed as input to the last convolution layer, which is further extended by residual connection.

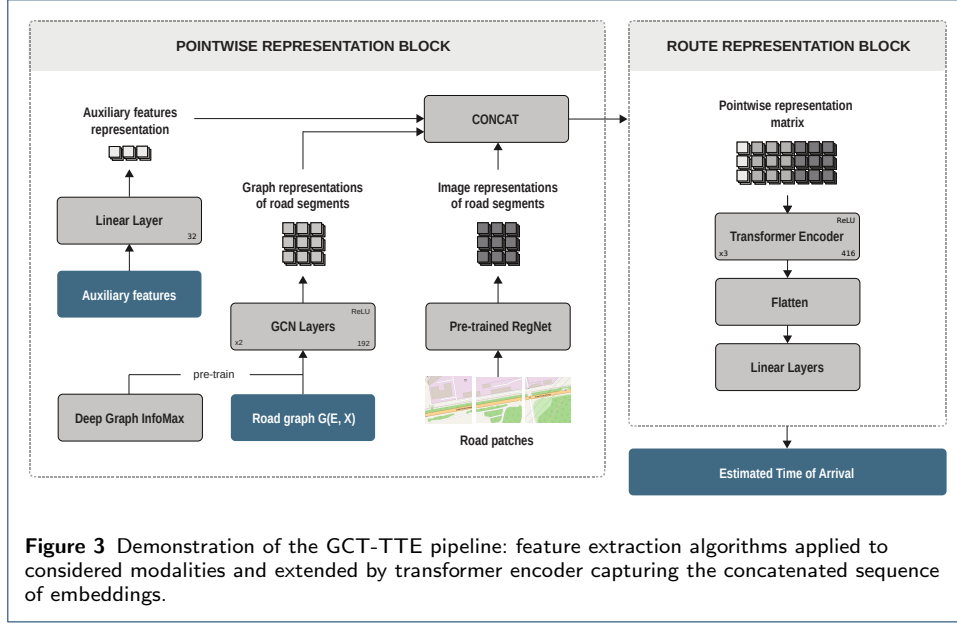
As the SEER models are capable of producing robust features that are well-suited for out-of-distribution generalization [28], we pre-trained RegNetY with the following autoencoder loss:

$$\mathcal{L}(W \times \text{RegNet}(X), f(X)) \rightarrow 0, \quad (2)$$

where  $\mathcal{L}$  is the binary cross-entropy function,  $f$  is an image flattening operator, and  $W$  is the projection matrix of learning parameters that maps model output to the flattened image.

#### Auxiliary encoder

Along with the map patches and graph elements, we apply additional features  $a^r$  corresponding to the temporal and weather data (e.g., trip hour, type of day, precipitation). The GCT-TTE model processes this part of the input with the help of



a trivial linear layer:

$$A^r = W a^r, \quad (3)$$

where  $W$  is a matrix of learning parameters.

### Graph encoder

The graph data is handled with the help of the graph convolutional layers defined as follows:

$$h_u^{(k)} = \text{ReLU} \left( W^{(k)} \text{AGG}_{v \in \mathcal{N}(u)} \left( \frac{h_v^{(k-1)}}{|\mathcal{N}_{uv}|} \right) \right), \quad (4)$$

where  $h_u^{(k)}$  is a  $k$ -hop embedding [29] of  $u \in V$ ,  $h_u^{(0)} = x_u$ ,  $W^{(k)}$  is a matrix of learning parameters of  $k$ 'th convolutional layer,  $\mathcal{N}(u)$  is a set of neighbour nodes of  $u$ ,  $\text{AGG}_{v \in \mathcal{N}(u)}$  is a sum aggregation function, and  $|\mathcal{N}_{uv}| = \sqrt{|\mathcal{N}(u)||\mathcal{N}(v)|}$ .

To accelerate the convergence of the GCT-TTE model, we pre-trained the weights of the graph convolutions by the Deep Graph InfoMax algorithm [30]. This approach optimizes the loss function that allows learning the difference between initial and corrupted embeddings of nodes:

$$\mathcal{L} = \frac{1}{N + M} \left( \sum_{i=1}^N E_{\mathcal{G}} \left[ \log(D(h_u, h_{\mathcal{G}})) \right] + \sum_{j=1}^M E_{\tilde{\mathcal{G}}} \left[ \log(1 - D(\tilde{h}_u, h_{\mathcal{G}})) \right] \right), \quad (5)$$

where  $h_u$  is an embedding of node  $u$  based on the initial graph  $\mathcal{G}$ ,  $\tilde{h}_u$  is an embedding of a node  $u$  from the corrupted version  $\tilde{\mathcal{G}}$  of the graph  $\mathcal{G}$ ,  $D$  corresponds to the discriminator function.

The final output of the pointwise block constitutes a concatenation of the weighted representations and auxiliary data for each route  $r$  with  $k$  segments:

$$P_r = \text{CONCAT}(\alpha \cdot H^r, (1 - \alpha) \cdot I^r, \beta \cdot A^r), \quad (6)$$

where  $H^r$  is the matrix of size  $k \times e_g$  of graph-based segment embeddings,  $I^r$  is the matrix of size  $k \times e_i$  obtained from a flattened RegNet output,  $\alpha$ ,  $(1 - \alpha)$ , and  $\beta$  correspond to the weight coefficients of specific modalities.

### Sequence representation block

To extract sequential features from the output of the pointwise representation block, it is fed to transformer encoder [31]. The encoder consists of two attention layers with a residual connection followed by a normalization operator. The multi-head attention coefficients are defined as follows:

$$\alpha_{i,j}^{(h)} = \text{softmax}_{w_j} \left( \frac{\langle W_{h,q}^T x_i, W_{h,k}^T x_j \rangle}{\sqrt{d_k}} \right), \quad (7)$$

where  $x_i, x_j \in P_r$ ,  $h$  is an attention head,  $d_k$  is a scale coefficient,  $W_{h,q}^T$  and  $W_{h,k}^T$  are query and key weight matrices,  $w_j$  is a vector of softmax learning parameters. The output of the attention layer will be:

$$u_i = \text{LayerNorm} \left( x_i + \sum_{h=1}^H W_{c,h}^T \sum_{j=1}^n \alpha_{i,j}^{(h)} W_{h,v}^T x_j \right), \quad (8)$$

where  $W_{h,v}^T$  is value weight matrix,  $H$  is a number of attention heads.

The final part of the sequence representation block corresponds to the flattening operator and several linear layers with the ReLU activation, which predict the travel time of a route.

## Results

In this section, we reveal the parameter dependencies of the model and compare the results of the considered baselines.

### Experimental setup

The experiments were conducted on 16 GPU Tesla V100. For the GCT-TTE training, Adam optimizer [32] was chosen with a learning rate  $5 \cdot 10^{-5}$  and batch size of 16. For better convergence, we apply the scheduler with patience equal to 10 epochs and 0.1 scaling factor. The training time for the final configuration of the GCT-TTE model is 6 hours in the case of Abakan and 30 for Omsk.

The established values of quality metrics were obtained from the 5-fold cross-validation procedure. As the measures of the model performance, we use mean absolute error (MAE), rooted mean squared error (RMSE), and 10% satisfaction rate (SR). Additionally, we compute mean absolute percentage error (MAPE) as it is frequently applied in related studies.

**Table 3** Path-blind models comparison

	Abakan				Omsk			
<i>Baseline \ Metric</i>	MAE	RMSE	MAPE	SR	MAE	RMSE	MAPE	SR
AVG	322.77	477.61	0.761	0.018	439.05	628.75	0.741	0.012
LR	262.33	456.63	1.169	9.527	416.81	593.01	1.399	7.187
GBDT	245.77	433.91	1.106	10.28	<b>209.99</b>	<b>372.11</b>	0.656	<b>17.72</b>
MURAT	<b>182.97</b>	<b>282.15</b>	0.685	10.77	285.72	444.74	0.856	9.997
GCT-TTE	221.71	337.59	<b>0.505</b>	<b>11.12</b>	376.74	590.93	<b>0.5486</b>	8.99

**Table 4** Path-aware models comparison

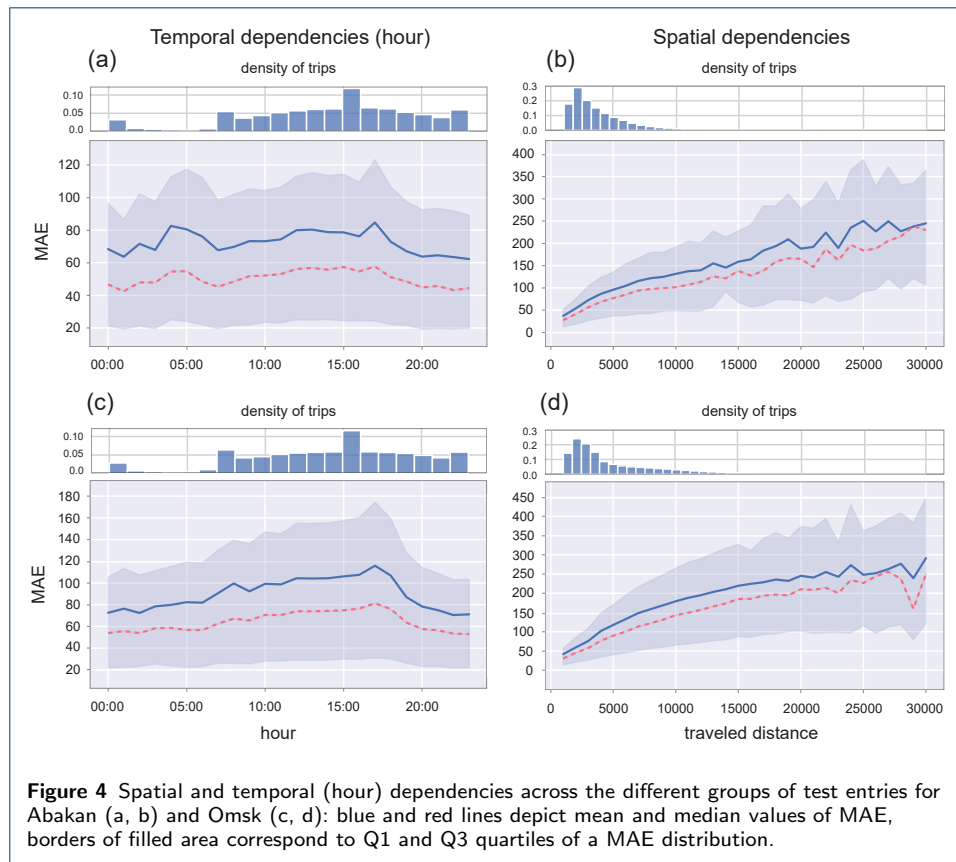
	Abakan				Omsk			
<i>Baseline \ Metric</i>	MAE	RMSE	MAPE	SR	MAE	RMSE	MAPE	SR
DeepIST	153.88	241.29	0.3905	18.08	256.50	415.16	0.6361	14.39
DeepTTE	111.03	174.56	0.2165	31.45	179.07	296.98	<b>0.1898</b>	34.03
GridLSTM	100.27	206.91	0.2202	30.74	135.74	257.18	0.2120	31.21
DeepI2T	97.99	201.33	<b>0.2128</b>	31.34	136.66	260.90	0.2124	31.23
WDR	97.22	190.09	0.2162	<b>31.98</b>	131.57	269.00	0.2039	33.34
GCT-TTE	<b>92.26</b>	<b>147.89</b>	0.2262	30.46	<b>107.97</b>	<b>169.15</b>	0.1961	<b>35.17</b>

### Models comparison and evaluation

The results regarding path-blind evaluation are depicted in Table 3. Neighbor average (AVG) and linear regression (LR) demonstrated the worst results among the trivial baselines as long as gradient boosted decision trees (GBDT) explicitly outperformed more complex models in the case of the largest city. The MURAT model achieved the best score for Abakan in terms of MAE and RMSE, while GCT-TTE has the minimum MAPE among all of the considered architectures.

Demonstrated variability of metric values makes the identification of the best model rather a hard task for a path-blind setting. The simplest models are still capable to be competitive regarding such architectures as MURAT, which was expected to perform tangibly better on both considered datasets. The results regarding GCT-TTE can be partially explained by its structure as it was not initially designed for a path-blind evaluation.

As can be seen in Table 4, the proposed solution outperformed baselines in terms of the RMSE value, which proves the rigidity of GCT-TTE towards large errors prevention. The comparison of MAE and RMSE for considered methods has shown a minimal gap between these metrics in the case of GCT-TTE for both cities, signifying the efficiency of the technique with respect to dataset size. Overall, the results have confirmed that GCT-TTE appeared to be a more reliable approach than the LSTM-based models: while MAPE remains approximately the same across top-performing architectures, GCT-TTE achieves significantly better MAE and RMSE values. Conducted computational experiments also indicated that DeepI2T and WDR have intrinsic problems with the convergence, while GCT-TTE demonstrates smoother training dynamics.



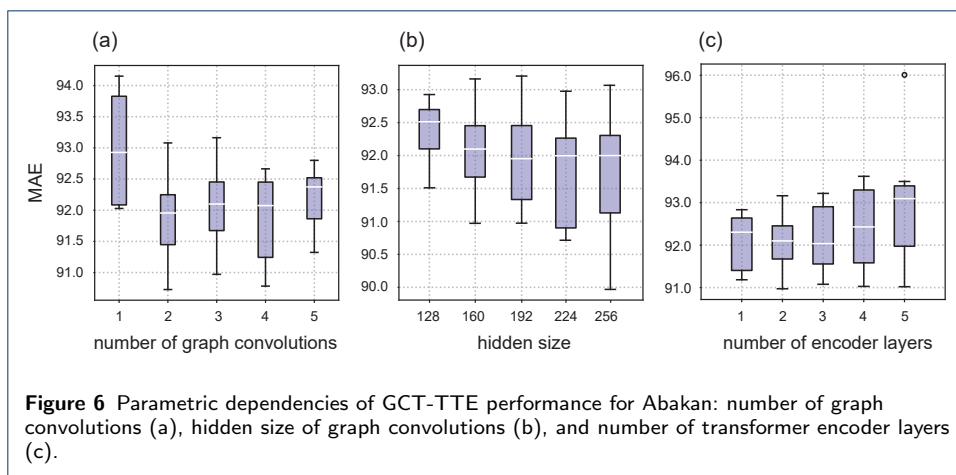
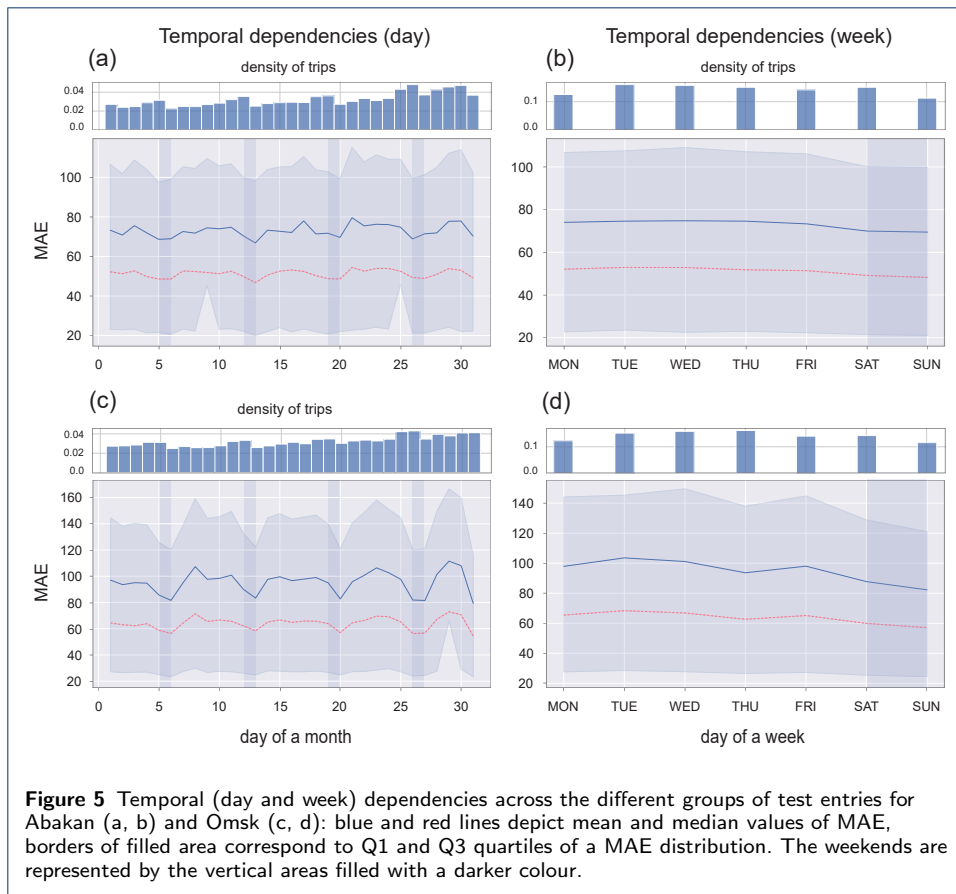
### Performance analysis

In the case of both datasets, dependencies between the travelled distance and obtained MAE on the corresponding trips reveal similar dynamics: as the path length increases, the error rate continues to grow, Figure 4(b, d). The prediction variance is inversely proportional to the number of routes in a particular length interval except for the small percentage of the shortest routes. The main difference between the MAE curves is reflected in the higher magnitudes of performance fluctuations in Abakan compared to Omsk.

The temporal dynamics of GCT-TTE errors exhibit rich nonlinear properties during a 24-hour period. The shape of the error curves demonstrates that our model tends to accumulate a majority of errors in the period between 16:00 and 18:00, Figure 4(a, c). This time interval corresponds to the end of the working day, which has a crucial impact on the traffic flow foreseeability.

Despite the mentioned performance outlier, the general behaviour of temporal dependencies allows concluding that GCT-TTE successfully captures the factors influencing the target value in the daytime. With the growing sparsity of data during night hours, it is still capable of producing relevant predictions for Omsk. In the case of Abakan, the GCT-TTE performance drop can be associated with a substantial reduction in intercity trips number (which emerged to be an easier target for the model).

Focusing on higher levels of seasonality, day- and week-based temporal dependencies of error demonstrate explicit periodical behaviour, Figure 5. The GCT-TTE



model performs better at the end of the week for both considered cities, with a pronounced error decrease in the case of Omsk. In contrast, the middle of the week (i.e. Wednesday for Abakan and Tuesday for Omsk) is the most challenging period, which has on average 12.48% higher MAE compared to Saturday and Sunday.

### Sensitivity analysis

In order to achieve better prediction quality, we extensively studied the dependencies between GCT-TTE parameters and model performance in the sense of the

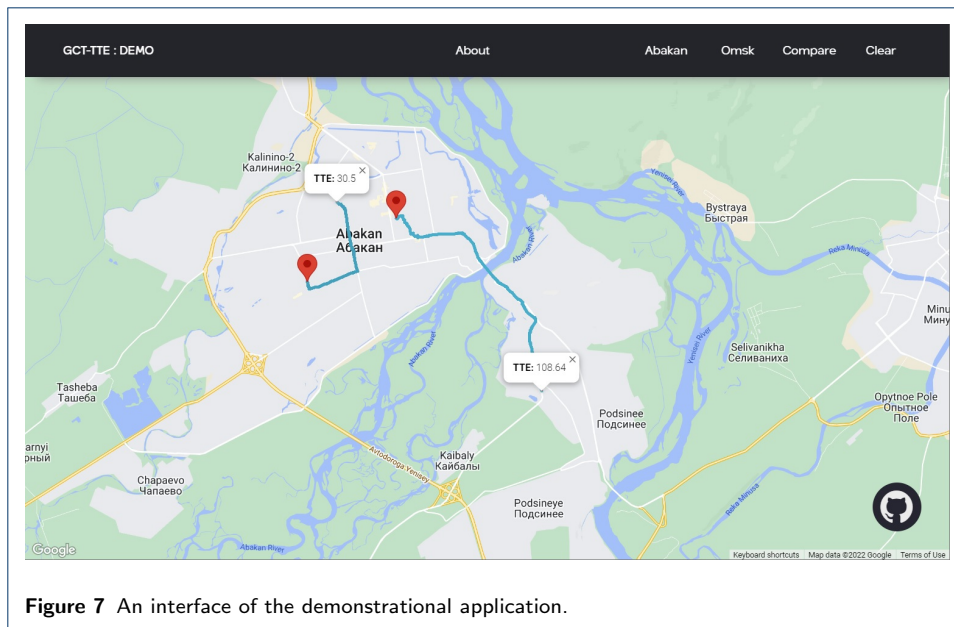


**Figure 7** An interface of the demonstrational application.

MAE metric. The best value for modality coefficient  $\alpha$  was 0.9, which reflects the significant contribution of graph data towards error reduction. For the final model, we utilized 2 graph convolutional layers with hidden size 192, Figure 6(a, b). The lack of aggregation depth can significantly reduce the performance of GCT-TTE, while the excessive number of layers has a less expressive negative impact on MAE. A similar situation can be observed in the case of the hidden size, which is getting close to a plateau after reaching a certain threshold value.

Along with the graph convolutions, we explored the configuration of the sequence representation part of GCT-TTE. Since the transformer block remains its main component, the computational experiments were focused on the influence of encoder depth on quality metrics, Figure 3(c). As it can be derived from the U-shaped dependency, the best number of attention layers is 3.

## Demonstration

In order to provide access to the inference of GCT-TTE, we deployed a demonstrational application<sup>[1]</sup> in a website format, Figure 7. The application's interface consists of a user guide, navigation buttons, erase button, and a comparison button. A potential user can construct and evaluate an arbitrary route by clicking on the map at the desired start and end points: the system's response will contain the shortest path and the corresponding value of the estimated time of arrival.

For additional evaluation of considered baselines, the limited number of predefined trajectories with known ground truth can also be requested. In this case, the response will contain three random trajectories from the datasets with associated predictions of WDR, DeepI2T, and GCT-TTE models along with the real travel time.

<sup>[1]</sup><http://gctte.online>

## Conclusion

In this paper, we introduced a multimodal transformer architecture for travel time estimation and performed an extensive comparison with the other existing approaches. Obtained results allow us to conclude that the transformer-based models can be efficiently utilized as sequence encoders in the path-aware setting. Our experiments with different data modalities revealed the superior importance of graphs compared to map patches. Such an outcome can be explained by the inheritance of main features between modalities where graph data represents the same properties more explicitly. In further studies, we intend to focus on the design of a more expressive image encoder as well as consider the task of path-blind travel time estimation, which currently remains challenging for the GCT-TTE model.

## Supplementary

### S1 – Features of the datasets

Graph node feature	Values	Description
Style	undefined, archway, crosswalk, stairway, bridge, overground way, invisible, normal, park path, park footpath, subway, pedestrian bridge, underground way, tunnel, living zone, ford	additional road segments categories
Road class	fake road, intra-quarter driveway, dirt road, other city street, main city street, highway, intercity road, federal highway, cycle path, walkway	general road segments categories
Length	$\mathbf{Z}_+$	length of a road segment in meters
Width	$\mathbf{Z}_+$	width of a road segment in meters
Def speed	{3, 15, 20, 60, 90}	speed limit on a road section in km/h
Lanes	{0, 1, 2, 3, 4, 5}	number of lanes in a road segment
Barrier	{0, 1}	defines the presence of road barriers
Payment flag	{0, 1}	defines a road segment as tol
Turn restrictions	{0, 1}	defines an ability to turn on a road section
Pedo offset	{0, 1}	defines the presence of crosswalk offsets
Bad road	{0, 1}	defines the condition of a road segment

Route feature	Values	Description
Nodes	$\{\hat{V} \subset V\}$	subset of nodes
Dist to a	$\mathbf{Z}_+$	length of a segment between actual start point and its projection on the first edge
Dist to b	$\mathbf{Z}_+$	length of a segment between actual end point and its projection on the last edge
Start point part	$\mathbf{Z}_+$	part of the first edge where the trip starts in meters
Finish point part	$\mathbf{Z}_+$	part of the last edge where the trip ends in meters
Start UTC	$\mathbf{Z}_+$	start time of the trip in UTC format
Real time of arrival	$\mathbf{Z}_+$	trip duration in second
Real dist*	$\mathbf{Z}_+$	Actual traveled distance in meters
Rebuild count*	$\mathbf{Z}_+$	number of route rebuilds that corresponds to the destination change

## S2 – split algorithm

**Algorithm 2** Splitting long segment

---

```

1: function SPLIT( $p_1, p_2$ ) ▷ Two points [latitude, longitude]
2:    $route\_centers = []$ 
3:   while  $\rho(p_1, p_2) \geq 200$  do
4:      $a = [(p_1[0] + p_2[0])/2, (p_1[1] + p_2[1])/2]$ 
5:     while  $\rho(x, a) \geq 200$  do
6:        $a = [(p_1[0] + a[0])/2, (p_1[1] + a[1])/2]$ 
7:     end while
8:      $route\_centers \leftarrow a$ 
9:      $p_1 = a$ 
10:  end while
11:   $route\_centers \leftarrow [(p_1[0] + p_2[0])/2, (p_1[1] + p_2[1])/2]$  ▷ Taking the middle of the final
    segment
12:  return  $route\_centers$ 
13: end function

```

---

## S3 – collect algorithm

**Algorithm 3** Calculating an overall centroid of densely spaced points

---

```

1: function COLLECT( $p_1, p_2, index$ )
2:    $center = [0, 0]$ 
3:    $i = index$ 
4:    $k = 2$ 
5:   while  $(i + k < len(path))$  and  $(\rho(path[i], path[i + k]) < 200)$  do
6:      $k = k + 1$ 
7:   end while
8:   for each  $m \in [0, \dots, k)$  do
9:      $center[0] = center[0] + path[i + m][0]$ 
10:     $center[1] = center[1] + path[i + m][1]$ 
11:   end for
12:    $center[0] = \frac{center[0]}{k}$ 
13:    $center[1] = \frac{center[1]}{k}$ 
14:
15:   return  $(center, k - 1)$  ▷ Returns both values at once
16: end function

```

---

## S4 – Learning &amp; model parameters for the path-aware approaches

Name	Optimizer hyperparameters	Model hyperparameters
DeepST	lr = 0.000001, optimizer = Adam, scheduler = ReduceLROnPlateau, scheduler_patience=1000	G1 = 0.1, G2 = 0.1, G3 = 0.01, max_seq_len = 15
DeepTTE	lr = 0.0005, optimizer = AdamW, batch_size=4	num_filter = 32, pooling_method = "attention", kernel_size = 6, alpha = 0.65, num_final_fcs = 3, final_fc_size = 128
DeepI2T	lr = 0.01, optimizer = SGD, scheduler = ReduceLROnPlateau, scheduler_regime = 'min', scheduler_patience=2, scheduler_factor=0.5, batch_size=64	without_direction = False, without_conv = False, without_line = False, without_flow = False, LSTM_hidden_size = 338, bidirectional = False, LINE_embedding_size = 100
WDR	lr=0.000001, optimizer = Adam, batch_size=32	hidden_size = 100, num_layers = 1, bidirectional=False, deep_input_size = 16, wide_input_size = 528
MURAT	lr = 0.01, optimizer = Adam	alpha = 0.2, num_epochs = 100

**Declarations****Ethics approval and consent to participate**

Not applicable.

**Consent for publication**

Not applicable.

**Availability of data and materials**

Considered models and datasets are available in the project's GitHub repository.

**Competing interests**

The authors declare that they have no competing interests.

**Funding**

Not applicable.

**Authors contributions**

V.M., V.C., and A.I.: Software, Data curation, Validation, Visualization; V.P.: Software, Visualization, Conceptualization, Methodology, Writing (original draft); N.S.: Conceptualization, Methodology, Supervision, Writing (review & editing).

**Acknowledgements**

Authors are grateful to Vladislav Zamkovy for the help with application deployment.

**Author details**

<sup>1</sup>PJSC Sberbank, Vavilova Street, 117312 Moscow, Russia. <sup>2</sup>University of Amsterdam, Science Park 904, 1098 XH Amsterdam, The Netherlands. <sup>3</sup>National University of Science and Technology "MISIS", Lenin Avenue 4, 119049 Moscow, Russia. <sup>4</sup>Artificial Intelligence Research Institute, Nizhniy Susalny Lane 5, 105064 Moscow, Russia.

**References**

- Jenelius, E., Koutsopoulos, H.: Travel time estimation for urban road networks using low frequency probe vehicle data. *Transportation Research Part B: Methodological* **53**, 64–81 (2013)
- Wu, X., Roy, U., Hamidi, M., Craig, B.: Estimate travel time of ships in narrow channel based on ais data. *Ocean Engineering* **202**, 106790 (2020)
- Xuegang, J., Ban, X.J., Li, Y., Skabardonis, A., Margulici, J.: Performance evaluation of travel time estimation methods for real-time traffic applications. *Intelligent Transportation Systems Journal* **14**, 54–67 (2010)
- Salehi, S., Mahmoudabadi, A.: Estimating the reliability of travel time on railway networks for freight transportation. *Urban Studies and Public Administration* **1**, 75 (2018). doi:10.22158/usp.v1n1p75
- Shi, C., Chen, B.Y., Li, Q.: Estimation of travel time distributions in urban road networks using low-frequency floating car data. *ISPRS International Journal of Geo-Information* **6**(8) (2017)
- Navarro-Espinoza, A., López-Bonilla, O.R., García-Guerrero, E.E., Tlelo-Cuautle, E., López-Mancilla, D., Hernández-Mejía, C., Inzunza-González, E.: Traffic flow prediction for smart traffic lights using machine learning algorithms. *Technologies* **10**(1) (2022). doi:10.3390/technologies10010005
- Wang, Q., Xu, C., Zhang, W., Li, J.: GraphTTE: Travel time estimation based on attention-spatiotemporal graphs. *IEEE Signal Processing Letters* **28**, 239–243 (2021)
- Derrow-Pinion, A., She, J., Wong, D., Lange, O., Hester, T., Perez, L., Nunkesser, M., Lee, S., Guo, X., Wiltshire, B., *et al.*: Eta prediction with graph neural networks in google maps. In: *Proceedings of the 30th ACM International Conference on Information & Knowledge Management*, pp. 3767–3776 (2021)
- Chu, K.-F., Lam, A.Y.S., Li, V.O.K.: Deep multi-scale convolutional lstm network for travel demand and origin-destination predictions. *IEEE Transactions on Intelligent Transportation Systems* **21**(8), 3219–3232 (2020). doi:10.1109/TITS.2019.2924971
- He, P., Jiang, G., Lam, S.-K., Sun, Y., Ning, F.: Exploring public transport transfer opportunities for pareto search of multicriteria journeys. *IEEE Transactions on Intelligent Transportation Systems* **23**(12), 22895–22908 (2022). doi:10.1109/TITS.2022.3194523
- Porvatov, V., Semenova, N., Chertok, A.: Hybrid graph embedding techniques in estimated time of arrival task. In: Benito, R.M., Cherifi, C., Cherifi, H., Moro, E., Rocha, L.M., Sales-Pardo, M. (eds.) *Complex Networks & Their Applications X*, pp. 575–586. Springer, Cham (2022)
- Wang, H., Tang, X., Kuo, Y.-H., Kifer, D., Li, Z.: A simple baseline for travel time estimation using large-scale trip data. *ACM Transactions on Intelligent Systems and Technology (TIST)* **10**(2), 1–22 (2019)
- Wang, Y., Zheng, Y., Xue, Y.: Travel time estimation of a path using sparse trajectories. In: *Proceedings of the 20th ACM SIGKDD International Conference on Knowledge Discovery and Data Mining. KDD '14*, pp. 25–34. Association for Computing Machinery, New York, NY, USA (2014)
- Fu, T.-y., Lee, W.-C.: Deepist: Deep image-based spatio-temporal network for travel time estimation. In: *Proceedings of the 28th ACM International Conference on Information and Knowledge Management. CIKM '19*, pp. 69–78. Association for Computing Machinery, New York, NY, USA (2019)
- Zhang, H., Wu, H., Sun, W., Zheng, B.: Deeptravel: a neural network based travel time estimation model with auxiliary supervision. In: *Proceedings of the 27th International Joint Conference on Artificial Intelligence*, pp. 3655–3661 (2018)
- Sun, Y., Fu, K., Wang, Z., Zhang, C., Ye, J.: Road network metric learning for estimated time of arrival. In: *2020 25th International Conference On Pattern Recognition (ICPR)*, pp. 1820–1827 (2021). IEEE
- Wang, Z., Fu, K., Ye, J.: Learning to estimate the travel time. In: *Proceedings of the 24th ACM SIGKDD International Conference on Knowledge Discovery and Data Mining. KDD '18*, pp. 858–866. Association for Computing Machinery, New York, NY, USA (2018)
- Cheng, H.-T., Koc, L., Harmsen, J., Shaked, T., Chandra, T., Aradhye, H., Anderson, G., Corrado, G., Chai, W., Ispir, M., *et al.*: Wide & deep learning for recommender systems. In: *Proceedings of the 1st Workshop on Deep Learning for Recommender Systems*, pp. 7–10 (2016)
- Hochreiter, S., Jürgen Schmidhuber, J., Elvezia, C.: Long short-term memory. *Neural Computation* **9**(8), 1735–1780 (1997)

20. Wang, D., Zhang, J., Cao, W., Li, J., Zheng, Y.: When will you arrive? estimating travel time based on deep neural networks. In: AAAI 2018 (2018)
21. Lan, W., Xu, Y., Zhao, B.: Travel time estimation without road networks: An urban morphological layout representation approach. In: Proceedings of the 28th International Joint Conference on Artificial Intelligence. IJCAI'19, pp. 1772–1778. AAAI Press, ??? (2019)
22. Tang, J., Qu, M., Wang, M., Zhang, M., Yan, J., Mei, Q.: Line: Large-scale information network embedding. In: Proceedings of the 24th International Conference on World Wide Web, pp. 1067–1077 (2015)
23. Liu, F., Yang, J., Li, M., Wang, K.: Mct-tte: Travel time estimation based on transformer and convolution neural networks. *Scientific Programming* **2022**, 3235717 (2022)
24. Semenova, N., Porvatov, V., Tishin, V., Sosodka, A., Zamkovoy, V.: Logistics, graphs, and transformers: Towards improving travel time estimation. arXiv preprint arXiv:2207.05835 (2022)
25. Shen, Y., Jin, C., Hua, J., Huang, D.: Ttpnet: A neural network for travel time prediction based on tensor decomposition and graph embedding. *IEEE Transactions on Knowledge and Data Engineering* **34**(9), 4514–4526 (2022). doi:[10.1109/TKDE.2020.3038259](https://doi.org/10.1109/TKDE.2020.3038259)
26. Fan, S., Li, J., Lv, Z., Zhao, A.: Multimodal traffic travel time prediction. In: 2021 International Joint Conference on Neural Networks (IJCNN), pp. 1–9 (2021). doi:[10.1109/IJCNN52387.2021.9533356](https://doi.org/10.1109/IJCNN52387.2021.9533356)
27. Radosavovic, I., Kosaraju, R.P., Girshick, R., He, K., Dollár, P.: Designing network design spaces. In: Proceedings of the IEEE/CVF Conference on Computer Vision and Pattern Recognition (CVPR) (2020)
28. Goyal, P., Duval, Q., Seessel, I., Caron, M., Misra, I., Sagun, L., Joulin, A., Bojanowski, P.: Vision Models Are More Robust And Fair When Pretrained On Uncurated Images Without Supervision. arXiv (2022)
29. Kipf, T.N., Welling, M.: Semi-Supervised Classification with Graph Convolutional Networks. arXiv (2016)
30. Veličković, P., Fedus, W., Hamilton, W.L., Liò, P., Bengio, Y., Hjelm, R.D.: Deep Graph Infomax. In: International Conference on Learning Representations (2019)
31. Vaswani, A., Shazeer, N., Parmar, N., Uszkoreit, J., Jones, L., Gomez, A.N., Kaiser, L.u., Polosukhin, I.: Attention is all you need. In: Guyon, I., Luxburg, U.V., Bengio, S., Wallach, H., Fergus, R., Vishwanathan, S., Garnett, R. (eds.) *Advances in Neural Information Processing Systems*, vol. 30. Curran Associates, Inc., ??? (2017)
32. Kingma, D., Ba, J.: Adam: A method for stochastic optimization. International Conference on Learning Representations (2014)